Supporting Information

Hierarchical Structural Evolution of Zn_2GeO_4 in Binary Solvent and its Effect on Li-ion Storage Performance

Wei Liu,[†] Tengfei Zhou,[‡] Yang Zheng,[‡] Jianwen Liu,[†] Chuanqi Feng,[†] Yue Shen,[§] Yunhui Huang,[§] and Zaiping Guo,*[,†,‡]

[†]Hubei Collaborative Innovation Center for Advanced Organic Chemical Materials, Ministry-of-Education Key Laboratory for Synthesis and Applications of Organic Functional Molecules, Hubei University, Wuhan 430062, China.

[‡]Institute for Superconducting and Electronic Materials, School of Mechanical, Materials, and Mechatronics Engineering, University of Wollongong, North Wollongong, NSW 2500, Australia.

[§]State Key Laboratory of Material Processing and Die & Mould Technology, School of Materials Science and Engineering, Huazhong University of Science and Technology, Wuhan, Hubei 430074, China.

*Correspondence to: zguo@uow.edu.au (ZPG)

Materials Characterization. The crystalline phases of the resultant materials were characterized by powder X-ray diffraction (XRD, PANalytical B.V.), which was carried out using Cu Kα radiation (λ = 1.5406 Å) from 2θ = 10° to 80°. The morphology and microstructure were observed with a field emission scanning electron microscope (FE-SEM, Nova NanoSEM 450) and a field emission transmission electron microscopy (FE-TEM; Tecnai G2 F30). Raman spectroscopy was collected on an inVia Reflex (Renishaw) spectrometer using a 785 nm laser. X-ray photoelectron spectra (XPS) were recorded on a VG MultiLab 2000 system with a monochromatic A1 Kα X-ray source (ThermoVG Scientific).

Electrochemical Measurements. The electrodes were fabricated by mixing the active material, Super P, and Na-carboxymethyl cellulose (CMC) in a weight ratio of 8:1:1 in deionized water, followed by pasting the slurry onto copper foil by scraping with a knife. After drying in vacuum at 80 °C for 24 h, it was cut into small pieces with a diameter of 8 mm. The 2032 cells were assembled in an argon filled glovebox, using lithium metal as the counter electrode, Celgard 2300 membrane as the separator, and 1 M LiPF6 dissolved in ethylene carbonate, diethyl carbonate and dimethyl carbonate (EC-DEC-DMC) mixed solvent (1:1:1 by weight) as the electrolyte. The electrochemical performances were recorded on a Land battery measurement system (Wuhan, China) with a cut-off voltage of 0.01–2.80 V vs. Li/Li^+ at room temperature. Cyclic voltammetry (CV) curves were recorded on an electrochemical workstation (CHI 660d) at a scan rate of 0.1 mV s^{-1} between 0.01 and 2.80 V.

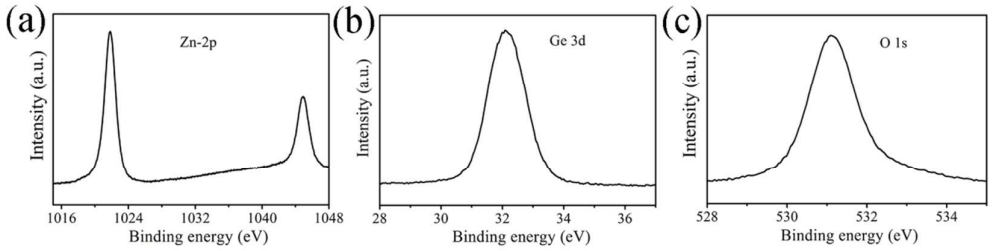

Figure S1. XPS spectra of ZGO-2: a) Zn 2p peak, b) Ge 3d peak, and c) O 1s peak.

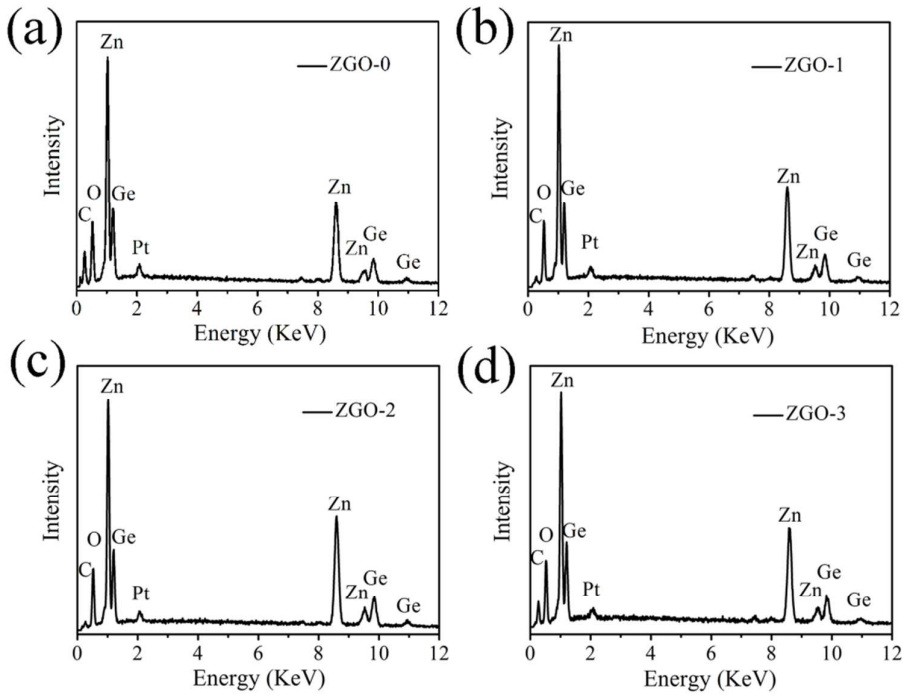

Figure S2. EDS spectra of ZGO-0 (a), ZGO-1 (b), ZGO-2 (c), and ZGO-3 (d), respectively. The microanalyses confirmed the presence of Zn, Ge, and O species, as well as signals of C and Pt, which were generated from the carbon conductive tape and by Pt sputtering to decrease the charging effects under the SEM-imaging conditions.

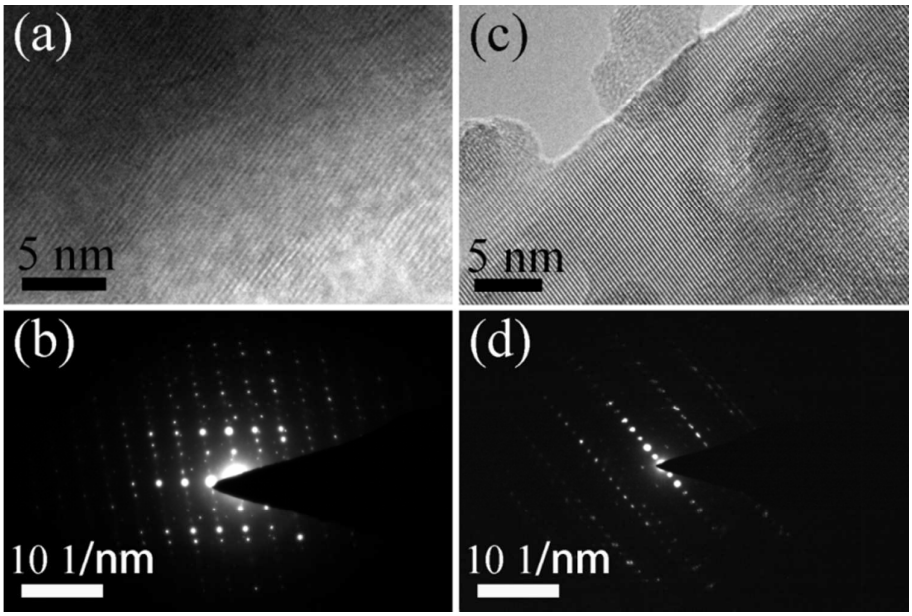

Figure S3. HRTEM images and corresponding FFT patterns of ZGO-0 (a, b) and ZGO-2 (c, d), respectively.

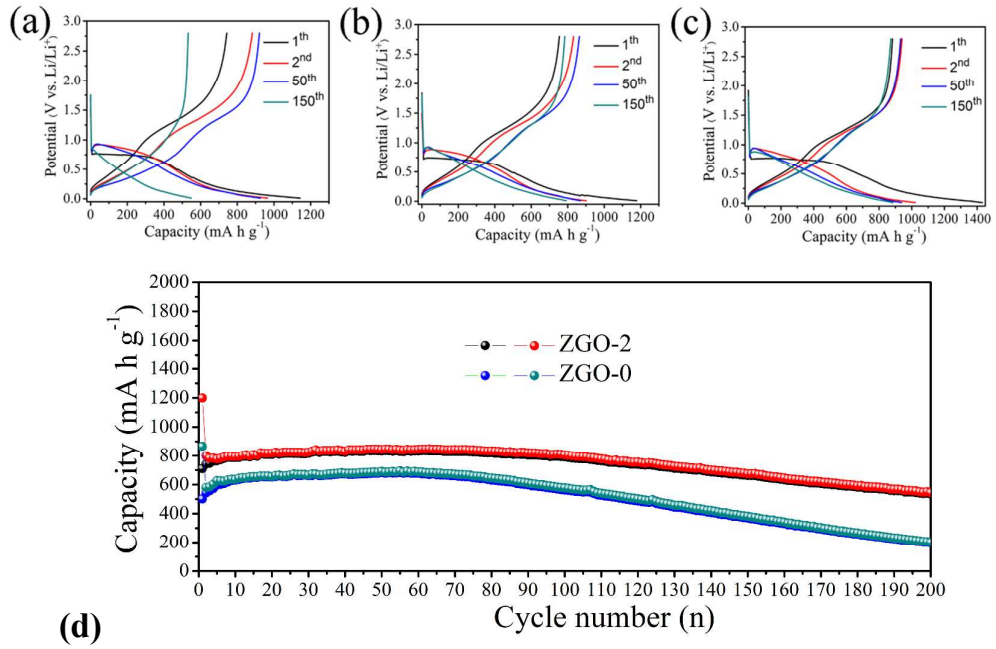

Figure S4. Discharge and charge profiles of ZGO-0 (a), ZGO-1 (b), and ZGO-3 (c) at a current density of 0.5 A g^{-1} for the 1st, 2nd, 50th, and 150th cycles, (d) Cycling performances of ZGO-0 and ZGO-2 at the charge/discharge current density of 1 A g^{-1} between 0.01 and 2.80 V.

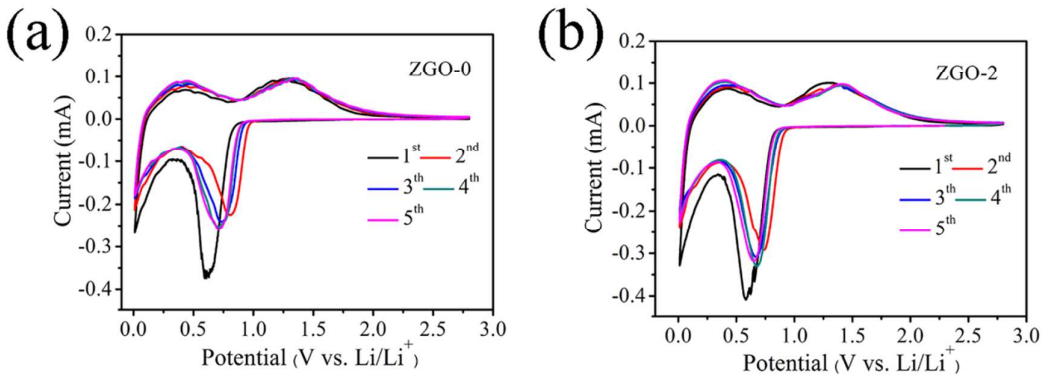

Figure S5. Cyclic voltammograms for the first 5 cycles of ZGO-0 (a), and ZGO-2 (b).

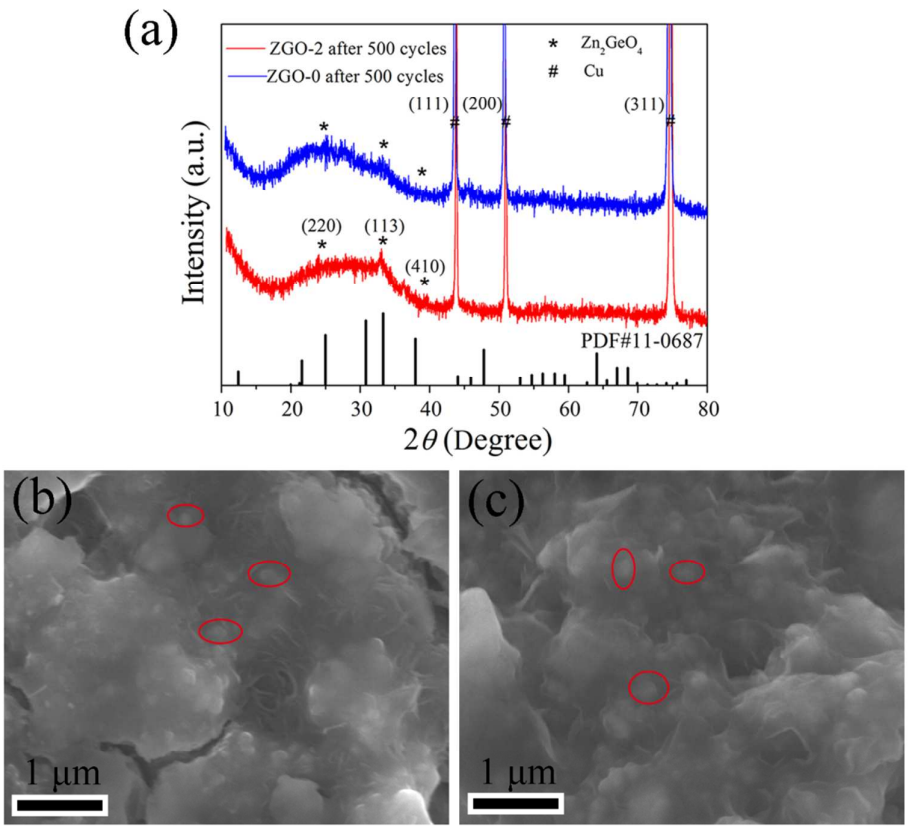

Figure S6. (a) X-ray diffraction patterns of the cycled ZGO-0 and ZGO-2 electrodes, and the cycled SEM images of ZGO-0 (b) and ZGO-2 (c) electrode.

Table S1. Comparison of the capacity of present work with rported Zn_2GeO_4-based materials.

Sample	Current density ($A\ g^{-1}$)	Cycle number (n)	Capacity ($mA\ h\ g^{-1}$)	Ref
Zn_2GeO_4 nanorods	0.4	100	616	[1]
Zn_2GeO_4 /N-doped graphene	0.1	100	1044	[2]
Zn_2GeO_4 hollow nanoparticles	0.2	60	1175	[3]
Amorphous Zn_2GeO_4 nanoparticles	0.4	500	1250	[4]
Zn_2GeO_4/g-C_3N_4 hybrids	0.2	140	1370	[5]
Coaxial Zn_2GeO_4 @ carbon nanowires	0.2	100	1112	[6]
Sandwiched Zn_2GeO_4−graphene oxide	0.2	100	1150	[7]
Mn-doped Zn_2GeO_4 nanosheets	0.1	100	1301	[8]
Interlaced porous Zn2GeO4 nanofibe	0.2	50	1084	[9]
Fascicular Zn_2GeO_4	0.5	160	1034	In this work

Reference

(1) Feng, J. K.; Lai, M. O.; Lu, L. Zn_2GeO_4 Nanorods Synthesized by Low-temperature Hydrothermal Growth for High-capacity Anode of Lithium Battery. *Electrochem. Commun.* **2011**, *13*, 287–289.

(2) Zou, F.; Hu, X.; Sun, Y.; Luo, W.; Xia, F.; Qie, L.; Jiang, Y.; Huang, Y. Microwave-induced In Situ Synthesis of Zn_2GeO_4/N-Doped Graphene Nanocomposites and Their Lithium-storage Properties. *Chem. Eur. J.* **2013**, *19* (19), 6027-6033.

(3) Feng, Y.; Li, X.; Shao, Z.; Wang, H. Morphology-dependent Performance of Zn_2GeO_4 as a High-Performance Anode Material for Rechargeable Lithium Ion Batteries. *J. Mater. Chem. A* **2015**. *3*(29), 15274-15279.

(4) Yi, R.; Feng, J. K.; Lv, D.; Gordin, M.; Chen, S.; Choi, D.; Wang, D. Amorphous Zn_2GeO_4 Nanoparticles as Anodes with High Reversible Capacity and Long Cycling Life for Li-ion Batteries. *Nano Energy* **2013**. *2*(4), 498-504.

(5) Li, X.; Feng, Y.; Li, M.; Li, W.; Wei, H.; Song, D. Smart Hybrids of Zn_2GeO_4 Nanoparticles and Ultrathin g-C_3N_4 Layers: Synergistic Lithium Storage and Excellent Electrochemical Performance. *Adv. Funct. Mater.* **2015**, *25*, 6858–6866.

(6) Chen, W.; Lu, L.; Maloney, S.; Yang, Y.; Wang, W. Coaxial Zn_2GeO_4@Carbon Nanowires Directly Grown on Cu Foils as High-performance Anodes for Lithium Ion Batteries. *Phys. Chem. Chem. Phys.* **2015**,*17*, 5109-5114

(7) Zou, F.; Hu, X.; Qie, L.; Jiang, Y.; Xiong, X.; Qiao, Y.; Huang, Y. Facile Synthesis of Sandwiched Zn_2GeO_4-graphene Oxide Nanocomposite as a Stable and High-capacity Anode for Lithium-ion Batteries. *Nanoscale* **2014**. *6*(2), 924-930.

(8) Li, Q.; Miao, X.; Wang, C.; Yin, L. Three-dimensional Mn-doped Zn_2GeO_4 Nanosheet Array Hierarchical Nanostructures Anchored on Porous Ni Foam as Binder-free and Carbon-free Lithium-ion Battery Anodes with Enhanced Electrochemical Performance. *J. Mater. Chem. A* **2015**. *3*(42), 21328-21336.

(9) Wang, W.; Qin, J.; Cao, M. Structure Interlacing and Pore Engineering of Zn_2GeO_4 Nanofibers for Achieving High Capacity and Rate Capability as an Anode Material of Lithium Ion Batteries. *ACS Appl. Mater. Interfaces* **2016**, *8*, 1388–1397.